TISSUE ENGINEERING: Part A
Volume 16, Number 2, 2010

DOI: 10.1089/ten.tea.2009.0158

Self-Assembling Peptide Hydrogels Modulate *In Vitro* Chondrogenesis of Bovine Bone Marrow Stromal Cells

Paul W. Kopesky, Ph.D.,[1] Eric J. Vanderploeg, Ph.D.,[2] John S. Sandy, Ph.D.,[3]
Bodo Kurz, Ph.D.,[4] and Alan J. Grodzinsky, Sc.D.[2]

Our objective was to test the hypothesis that self-assembling peptide hydrogel scaffolds provide cues that enhance the chondrogenic differentiation of bone marrow stromal cells (BMSCs). BMSCs were encapsulated within two unique peptide hydrogel sequences, and chondrogenesis was compared with that in agarose hydrogels. BMSCs in all three hydrogels underwent transforming growth factor-β1-mediated chondrogenesis as demonstrated by comparable gene expression and biosynthesis of extracellular matrix molecules. Expression of an osteogenic marker was unchanged, and an adipogenic marker was suppressed by transforming growth factor-β1 in all hydrogels. Cell proliferation occurred only in the peptide hydrogels, not in agarose, resulting in higher glycosaminoglycan content and more spatially uniform proteoglycan and collagen type II deposition. The G1-positive aggrecan produced in peptide hydrogels was predominantly the full-length species, whereas that in agarose was predominantly the aggrecanase product G1-NITEGE. Unique cell morphologies were observed for BMSCs in each peptide hydrogel sequence, with extensive cell–cell contact present for both, whereas BMSCs in agarose remained rounded over 21 days in culture. Differences in cell morphology within the two peptide scaffolds may be related to sequence-specific cell adhesion. Taken together, this study demonstrates that self-assembling peptide hydrogels enhance chondrogenesis compared with agarose as shown by extracellular matrix production, DNA content, and aggrecan molecular structure.

Introduction

Bone marrow stromal cells (BMSCs) have been widely used as a cell source for tissue engineering strategies aimed at resurfacing articular cartilage.[1–3] Significant progress has been made demonstrating the potential for BMSCs to undergo chondrogenesis and produce a cartilage-like extracellular matrix (ECM) when encapsulated in a variety of three-dimensional (3D) scaffolds including agarose,[4,5] alginate,[6] collagen type I,[7,8] gelatin/albumin,[9] and silk elastin,[10] but challenges in the use of BMSCs in the repair of cartilage defects still remain.[11,12] Improvements in BMSC chondrogenesis and eventual clinical use appear to require optimization of many factors. Among these is the current belief that the scaffold must provide the appropriate cell microenvironment and differentiation cues.[13] An ideal cartilage tissue engineering scaffold should be biocompatible, allow for cell adhesion, migration, and proliferation, and have sufficient porosity and hydration to permit nutrient and waste product flow. It should also stimulate production of an *in vivo*–like cartilage matrix with the appropriate cell-dependent turnover pathways. Finally it should be able to fill irregular defects, integrate effectively with the native recipient tissue, and degrade with the appropriate resorption kinetics.[11,13]

Self-assembling peptides are a relatively new class of molecules that have the capacity to form stable hydrogels and encapsulate viable cells for potential therapeutic applications.[14–16] One type of these peptides consists of short oligomers of alternating hydrophilic and hydrophobic residues that trigger self-assembly upon exposure to physiologic pH and ionic strength.[16] These peptides are completely synthetic, which avoids the potential pathogenicity of animal-derived materials.[17] Additionally, their rapid self-assembly enables cell encapsulation and irregular defect filling in both *in vitro* and *in vivo* applications. By varying the peptide sequence, hydrogel mechanical stiffness[18,19] and cell–scaffold adhesion[20] can be controlled, enabling the design of scaffolds optimized for use in cell-based cartilage,[21–23] liver,[24,25] and cardiovascular tissue repair.[26] We recently

[1]Department of Biological Engineering, MIT, Cambridge, Massachusetts.
[2]Center for Biomedical Engineering, MIT, Cambridge, Massachusetts.
[3]Department of Biochemistry, Rush University Medical Center, Chicago, Illinois.
[4]Anatomical Institute, Kiel, Germany.

completed a 12-week rabbit study and found that upon injection of peptide alone or with BMSCs into a critically sized defect in the trochlear groove, the peptide self-assembled into a gel scaffold *in situ* with sufficient mechanical integrity to withstand subsequent joint articulation.[27]

A successful cartilage repair therapy ultimately must generate a tissue with comparable ECM biochemistry and biomechanics to native tissue. Also, it will likely require that cues are provided to guide the BMSCs to closely mimic the temporal sequence of genetic, biochemical, and biophysical events in native chondrogenesis.[28,29] It is thus important that a detailed analysis of chondrogenesis for any cell-based therapy be performed *in vitro* as an assessment of its potential repair capacity *in vivo*. Measurements include chondrogenic gene expression at initial and subsequent timepoints,[30] characterization of early time-dependent changes in cell morphology,[7] quantification of cell content,[6] production and analysis of secreted ECM components,[5,31] and assessment of both anabolic and catabolic ECM processing.[32] Previous reports have used these analytical techniques to demonstrate how altering the cell microenvironment impacts BMSC chondrogenesis and neotissue formation.[6,30,33]

The objective of this study was to evaluate whether two different peptide hydrogels, KLD12 ($[KLDL]_3$) and RAD16-I ($[RADA]_4$), provided sequence-specific mechanical or adhesion cues that enhance transforming growth factor-β1 (TGF-β1)-stimulated chondrogenesis of BMSCs as compared with agarose hydrogel culture. Agarose was chosen as a reference because of its extensive use to study chondrocyte biology in 3D culture[34–36] and to evaluate progenitor cell differentiation.[4,22,23,32] Real-time reverse transcription–polymerase chain reaction (RT-PCR) was used to quantitatively assess expression of genes important for differentiation and ECM production. Neotissue cell content was measured by construct DNA content. The synthesis rate and accumulation of newly secreted ECM were also assessed biochemically. Changes in cytoskeleton morphology were characterized via F-actin imaging, and immunohistochemistry and immunoblotting were used to determine the type of ECM molecules and catabolic products. Timepoints for this study were chosen from 1–21 days of culture with the goal of understanding how peptide sequence impacts the initial stages of chondrogenesis.

Materials and Methods

Materials

Low-melting point agarose was from Invitrogen (Carlsbad, CA). KLD12 peptide with the sequence AcN-$(KLDL)_3$-CNH_2 was synthesized by the MIT Biopolymers Laboratory (Cambridge, MA) using an ABI Model 433A peptide synthesizer with 9H-fluoren-9-ylmethoxycarbonyl (FMOC) protection. RAD16-I peptide with the sequence $(RADA)_4$ was a gift of Puramatrix from 3DM (Cambridge, MA). All other materials were purchased from the suppliers noted below.

Cell isolation and expansion

BMSCs were isolated as described previously.[5] Briefly, bone marrow was harvested aseptically from three newborn bovine calves (Research 87, Marlborough, MA). Following centrifugation at 1000 *g* for 15 min, the cell pellet was washed in phosphate-buffered saline (PBS) and plated at 1×10^6 mononuclear cells/cm^2 in expansion medium consisting of low-glucose Dulbecco's modified Eagle's medium with 10% embryonic stem cell qualified fetal bovine serum (ES-FBS) (Invitrogen), 4-(2-hydroxyethyl)-l-piperazineethanesulfonic acid (HEPES), and Penicillin streptomycin amphotericin (PSA) (100 U/mL penicillin, 100 μg/mL streptomycin, and 250 ng/mL amphotericin) plus 1 ng/mL basic fibroblast growth factor (bFGF) (R&D Systems, Minneapolis, MN). Nonadherent cells were removed by a medium change after 48 h, and colonies were harvested with 0.05% trypsin/1 mM ethylenediaminetetraacetic acid (Invitrogen) after approximately 7 days (passage 0) and cryopreserved. Before peptide hydrogel encapsulation, cells were thawed and plated at $6\times10^3/cm^2$ in expansion medium plus 5 ng/mL Basic fibroblast growth factor (bFGF). After 3 days, cells were detached at $\sim3\times10^4$ cells/cm^2 (passage 1) and reseeded at $6\times10^3/cm^2$. This expansion was repeated during the subsequent 3 days after which cells were detached for encapsulation in 3D peptide hydrogels.

Hydrogel encapsulation and culture

BMSCs were encapsulated in 0.5% or 2% (w/v) low-melting point agarose, 0.35% (w/v) KLD12 peptide, or 0.5% (w/v) RAD16-I peptide at a concentration of 10^7 cells/mL. The different concentrations for the self-assembling peptides were chosen so that initially the hydrogels would have similar mechanical characteristics,[19,20] and 2% agarose was selected for comparison with previously published studies.[4,5,22,32] Hydrogel discs with 50 μL initial volume were cast in neutral-buffered, acellular agarose molds to initiate self assembly (Fig. 1) and cultured in high-glucose Dulbecco's modified Eagle's medium (Invitrogen) supplemented with 1% 1.0 mg/ml insulin, 0.55 mg/ml transferrin, 0.5 μg/ml sodium selenite, 50 mg/ml bovine serum albumin, and 470 μg/ml linoleic acid (ITS + 1) (Sigma-Aldrich, St. Louis, MO), 0.1 μM dexamethasone (Sigma-Aldrich), 37.5 μg/mL ascorbate-2-phosphate (Wako Chemicals, Richmond, VA), PSA, HEPES, Proline, and non-essential amino acids (NEAA), with (+TGF-

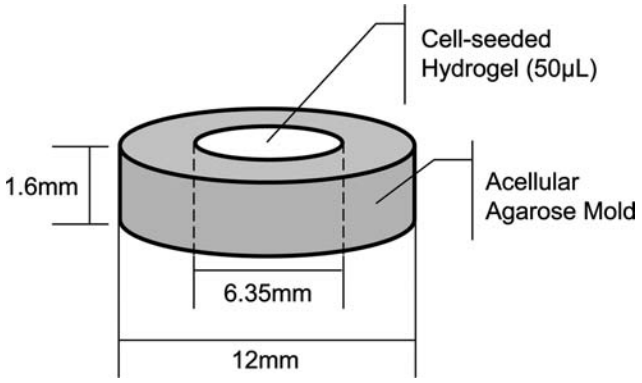

FIG. 1. Cell encapsulation and self-assembly mold. The acelluar-agarose annulus mold is made by injecting 2% agarose into a custom, autoclavable frame. Fifty microliters of cell-hydrogel suspension (bone marrow stromal cells [BMSCs] in RAD16-I, KLD12, or agarose) is then injected into the center to initiate self-assembly.

β1) or without (Cntl) 10 ng/mL recombinant human TGF-β1 (R&D Systems), with medium changes every 2–3 days.

Histology and immunohistochemistry

Hydrogels were fixed in 10% neutral-buffered formalin overnight at 4°C. For F-actin staining, 3D hydrogel samples were sliced to ~700-μm thick and permeabilized in PBS with 0.1% Triton-X at room temperature for 1 h. Samples were washed two to three times with PBS and stained for 1 h at room temperature with Texas Red–conjugated phalloidin to show F-actin fibers and Hoechst dye to observe cell nuclei. Samples were washed two to three times with PBS and imaged with a Nikon Eclipse fluorescent microscope or with a Zeiss LSM510 confocal microscope. For ECM staining, formalin-fixed hydrogels were embedded in paraffin and sliced to 7 μm using a sledge microtome (Leitz, Wetzlar, Germany). Sections were deparaffinized, treated with 0.1% pepsin for 30 min, rinsed with tris buffered saline (TBS), treated with 0.6% H_2O_2 in methanol, and rinsed again with TBS. Samples were then treated with either mouse anti-collagen type II IgG (Clone CII C1, developmental studies hybridoma bank (DSHB), 1:1000 in TBS) or mouse anti-collagen type I IgG (diluted 1:1000 in TBS; Sigma-Aldrich) for 1 h.[37] After incubation with rabbit anti-mouse IgG (horseradish peroxidase conjugated, diluted 1:200 in TBS containing 1% bovine serum, P0260; Dako, Glostrup, Denmark) for 30 min, the sections were rinsed and incubated for 30 min with goat anti-rabbit IgG (horseradish peroxidase conjugated, diluted 1:100 in TBS containing 1% bovine serum, P0448; Dako). Samples were stained with diaminobenzidine (DAB kit; Vector Laboratories, Burlingame, CA), and cell nuclei were counterstained with Mayer's hemalum. Finally, stained samples were embedded on microscope slides, using Aquatex (KGaA; Merck, Darmstadt, Germany). Additional sections were stained for proteoglycans using Toluidine Blue dye solution (0.0714% Toluidine Blue, Merck; 0.0714% pyronin Y, Fluka, Basel, Switzerland; and borax [0.143% di-sodium-tetra-borate], Merck) for 6 min as previously described.[21] For cell adhesion and spread area analyses, soluble KLD12 or RAD16-I (500 μg/mL in tissue culture water) was incubated overnight at 37°C in nontreated polystyrene culture plates. Plates were washed thoroughly with water and then incubated for at least 1 h with the ITS+ media described above. BMSCs at 1.2×10^4 cells/cm^2 were cultured for 2 h in TGF-β1-containing medium before being fixed and processed for cytoskeletal imaging as described above. Five random fields were imaged using a Nikon Eclipse fluorescent microscope, and the cell area and number of cells per field were measured with the Matlab Image Processing Toolbox (The MathWorks, Natick, MA).

Real-time RT-PCR

RNA was extracted as described previously.[38] BMSC-seeded hydrogel discs were flash frozen in liquid nitrogen, pulverized, and homogenized in TRIzol reagent (Invitrogen). RNA was extracted using an RNeasy Mini Kit (Qiagen, Valencia, CA) and quantified using a Nanodrop 1000 Spectrophotometer (Agilent Technologies, Santa Clara, CA). Absorbance measurements at 260 nm were used to determine the RNA concentration, and 1 μg of each sample was reverse transcribed using the AmpliTaq-Gold Reverse Transcription Kit (Applied Biosystems, Foster City, CA). Real-time RT-PCR was performed using the Applied Biosystems 7900HT and SYBR Green Master Mix (Applied Biosystems). Expression of type I collagen, type II collagen, aggrecan, SOX9, osteocalcin, PPAR-γ, and 18S was quantified using previously published primer sequences.[6,38,39] For each timepoint and hydrogel sample, gene expression levels were first normalized by the corresponding 18S level for that sample and then normalized by levels expressed by BMSC samples taken immediately before hydrogel encapsulation (day 0).[40]

Biochemistry

During the final 24 h of culture at each timepoint, medium was additionally supplemented with 5 μCi/mL of ^{35}S-sulfate and 10 μCi/mL of ^{3}H-proline to measure cellular biosynthesis of proteoglycans and proteins, respectively. Upon completion of culture, four 30-min rinses in excess nonlabeled sulfate and proline were performed for all samples to wash out free radiolabel. Hydrogels were then weighed wet, lyophilized, and weighed dry. Samples were digested in 0.25 mg/mL proteinase-K (Roche Applied Science, Indianapolis, IN) overnight at 60°C. Digested samples were assayed for total retained sulfated glycosaminoglycan (sGAG) content by 1.9-dimethylmethylene blue (DMMB) dye binding assay,[41] DNA content by Hoechst dye binding,[42] and radiolabel incorporation with a liquid scintillation counter. Conditioned culture medium collected throughout the study was also analyzed for sGAG content by DMMB dye binding.

Aggrecan extraction and Western analysis

Aggrecan was extracted from hydrogel discs and analyzed as described previously.[43] Hydrogel discs were saturated with PBS and Complete Protease Inhibitors (Roche) and frozen at −20°C until extraction. Gels were extracted for 48 h in 4 M guanidinium hydrochloride, deglycosylated, and the resulting digest was lyophilized. Samples were reconstituted, and 20 μg sGAG/lane was run on a 4–15% Tris–HCl gel at 100 V for 1 h. Proteins were transferred to a nitrocellulose membrane and probed with affinity-purified antibodies for aggrecan G1 domain (JSCATEG)[43] or to a polyvinylidene fluoride (PVDF) membrane and probed with a monoclonal antibody for the aggrecanase-generated NITEGE neoepitope (kindly provided by Carl Flannery and Wyeth, Inc., Cambridge, MA).[44]

Statistical analysis

All biochemical and hydrogel mass data were reported as mean ± standard error of the mean with four samples from each of the three animals ($n = 12$). RT-PCR results are reported as mean ± standard error of the mean using pooled samples from $n = 3$ animals. Data were analyzed by a mixed model of variance with animal as a random factor. Residual plots were constructed for dependent variable data to test for normality and data were transformed if necessary to satisfy this assumption. *Post hoc* Tukey tests for significance of pairwise comparisons were performed with a threshold for significance of $p < 0.05$.

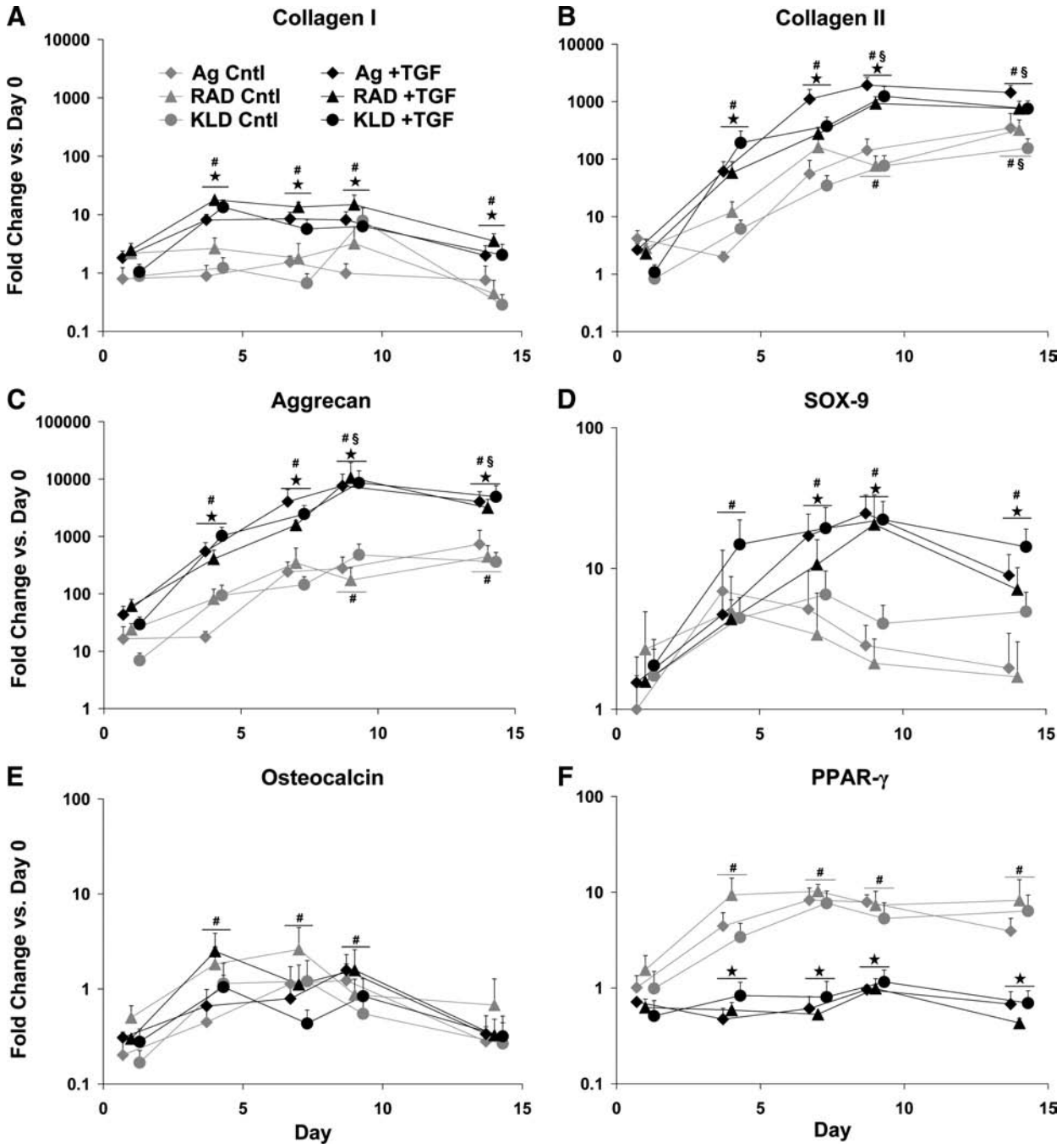

FIG. 2. Gene expression of BMSCs relative to passage 2, monolayer cells at day 0; cultured in control (Cntl) or transforming growth factor-β1 (TGF-β1)-supplemented (+TGF) medium and encapsulated in agarose (Ag), RAD16-I (RAD), or KLD12 (KLD). (**A**) Type I collagen, (**B**) type II collagen, (**C**) aggrecan, (**D**) SOX-9, (**E**) osteocalcin, and (**F**) PPAR-γ. All scaffolds were measured at the same timepoints, but offset for readability. Values are shown as mean + standard error of the mean; $n = 3$ animals; ⋆ versus Cntl medium; # or § versus day 1 or 4, respectively; $p < 0.05$.

Results

Chondrogenic, osteogenic, and adipogenic gene expression

Evidence that chondrogenesis occurred in all three hydrogels was provided by the upregulation of three cartilage-associated genes, type II collagen, aggrecan, and SOX-9 (Fig. 2B–D). As expected, TGF-β1 supplementation stimulated >100-fold upregulation of type II collagen and >1000-fold upregulation of aggrecan by day 4, with maximum upregulation at day 9 of >1000-fold and nearly 10,000-fold for type II collagen and aggrecan, respectively. In contrast, type I collagen, which is expressed by undifferentiated BMSCs and early in chondrogenesis,[29] was upregulated just 10-fold by day 4 with no further significant upregulation detected (Fig. 2A). Upregulation of type II collagen and aggrecan also occurred in control medium, but the magnitude was 10- to 100-fold lower than with TGF-β1 (Fig. 2B, C). No upregulation of type I

collagen or SOX-9 was seen in control medium. In all cases, these data showed no differences among the scaffolds, resulting in a similar overall gene expression pattern.

Neither osteogenic nor adipogenic gene expression was observed in any of the scaffolds. No significant differences were seen among scaffolds or medium conditions for osteocalcin, a marker for osteogenesis. At day 1, osteocalcin was downregulated by nearly fourfold (Fig. 2E), but returned to baseline on days 4 through 9, and finally dropped again on day 14 to an average of threefold below day 0 levels. PPAR-γ expression, a marker for adipogenesis, was upregulated in control medium at days 4, 7, 9, and 14 by ~fivefold in all three scaffolds (Fig. 2F); however, the addition of TGF-β1 reduced its expression to nearly baseline levels at all timepoints.

Hydrogel DNA content, sGAG content, and ECM biosynthesis

Increases in DNA content were stimulated by TGF-β1-supplemented medium for both peptide hydrogels, but not in agarose, throughout the entire culture period (Fig. 3A, $p < 0.05$). This resulted in significantly higher DNA content for RAD16-I peptide than for agarose at all timepoints

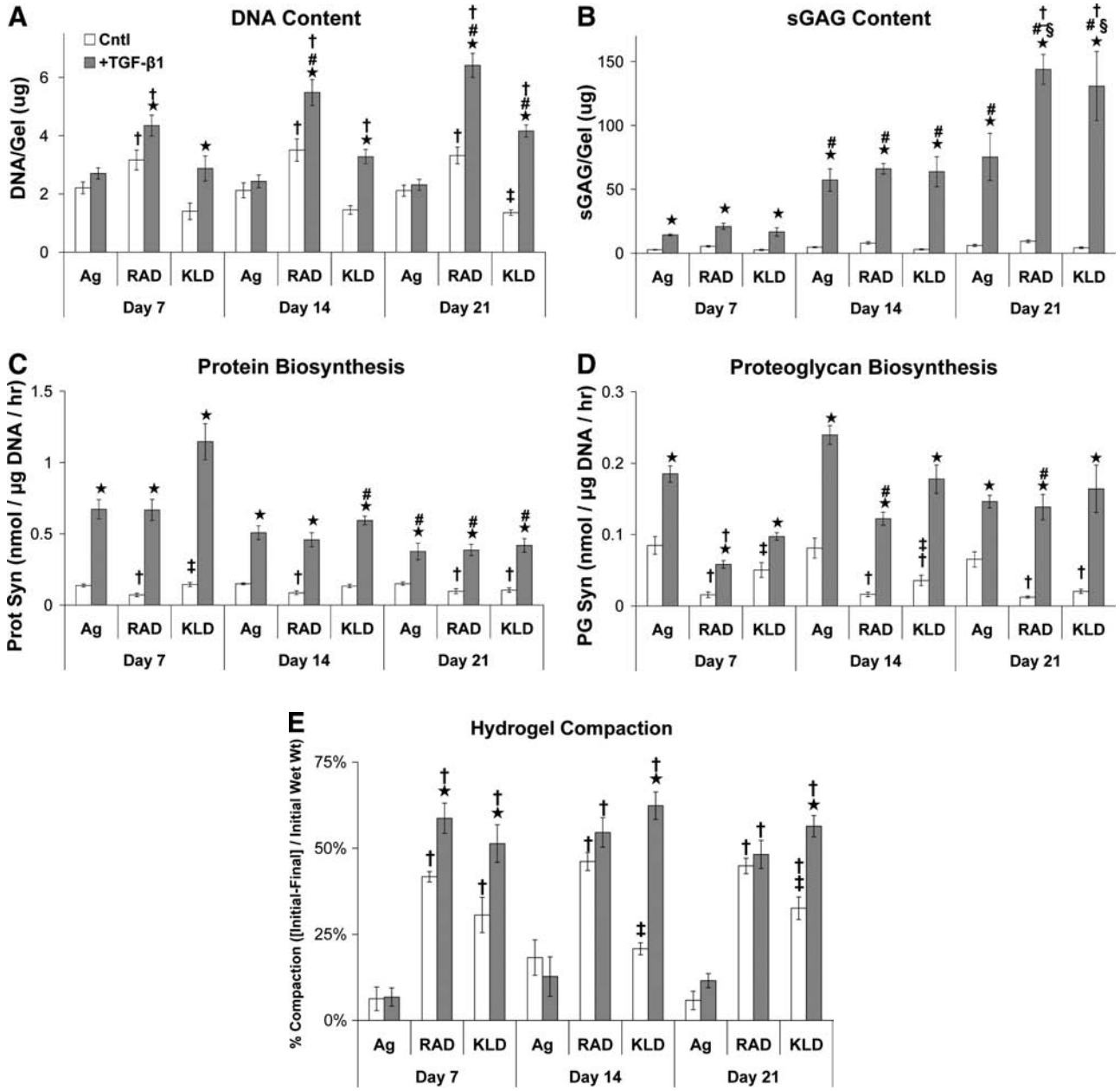

FIG. 3. Hydrogel biochemistry and extracellular matrix biosynthesis rates cultured in control (Cntl) or TGF-β1-supplemented (+TGF) medium and encapsulated in agarose (Ag), RAD16-I (RAD), or KLD12 (KLD). (**A**) DNA content, (**B**) sulfated glycosaminoglycan (sGAG) content, (**C**) protein biosynthesis, (**D**) proteoglycan biosynthesis, and (**E**) hydrogel compaction. Values are shown as mean ± standard error of the mean; $n = 12$ (4 gels×3 animals); ⋆ versus Cntl medium; # or § versus day 7 or 14, respectively; † or ‡ versus agarose or RAD16-I, respectively; $p < 0.05$.

($p < 0.001$) and higher DNA content for KLD12 than for agarose cultures at days 14 and 21 ($p < 0.001$). In addition, DNA content increased with time for both RAD16-I and KLD12 discs cultured in TGF-β1-supplemented medium resulting in significantly higher DNA content at day 21 versus day 7 ($p < 0.001$).

TGF-β1 stimulated a ~fivefold increase in sGAG content of all scaffolds at day 7 (Fig. 3B, $p < 0.001$) and a >10-fold increase at days 14 and 21 ($p < 0.001$) relative to controls. sGAG content increased with time for all three hydrogels through day 14 ($p < 0.001$). However, sGAG content only increased from day 14 to day 21 for the RAD16-I and KLD12 peptide hydrogels ($p < 0.001$) resulting in nearly twofold higher sGAG content for both peptides compared with agarose ($p < 0.005$). The percentage of sGAG retained in agarose hydrogels decreased with time in culture and was significantly lower compared with RAD16-I or KLD12 peptides at day 21 (Table 1, $p < 0.001$). In contrast, both RAD16-I and KLD12 peptides maintained constant sGAG retention throughout the culture period (Table 1) with modestly higher retention levels for RAD16-I peptide compared with KLD12 ($p < 0.05$).

Protein biosynthesis rates normalized to DNA content were four- to ninefold higher with TGF-β1 supplementation throughout the entire culture period (Fig. 3C, $p < 0.001$), and decreased with time by a factor of 2–3 for day 21 versus day 7 in all three hydrogels ($p < 0.005$). No differences in protein biosynthesis were seen among the three hydrogels. TGF-β1 stimulated 2- to 10-fold higher ^{35}S-proteoglycan biosynthesis rates at all timepoints in all three hydrogels (Fig. 3D, $p < 0.01$). Surprisingly (given the higher final sGAG content of the peptide hydrogels), ^{35}S-proteoglycan biosynthesis, on a per-DNA basis, was threefold higher for agarose than for RAD16-I peptide on day 7 ($p < 0.001$). However, proteoglycan biosynthesis increased in RAD16-I peptide by day 14 ($p < 0.05$) (when proliferation had essentially stopped), and no significant differences were seen among the three hydrogels in TGF-β1-supplemented medium at days 14 or 21.

Hydrogel wet weights and compaction

BMSCs compacted both peptide hydrogels 50–60% within the first week of culture in the presence of TGF-β1 as assessed by changes in wet mass (Fig. 3E). No further compaction was observed after 1 week. In control medium, compaction of both peptide hydrogels was 30–45% in the first week with no further compaction at later timepoints. No compaction was observed in 2% agarose hydrogels in either medium condition. However, in a separate experiment, when the agarose hydrogel concentration was reduced from 2% to 0.5% w/v, BMSCs with TGF-β1 compacted hydrogels by 69% in the first week with no further compaction at later timepoints (data not shown).

Table 1. Percent Sulfated Glycosaminoglycan Retained in Hydrogels Cultured with Transforming Growth Factor-β1

	Day 7	*Day 14*	*Day 21*
Agarose	62 ± 3	59 ± 2	$44 \pm 3^{a,b}$
RAD16-I	80 ± 4^{c}	74 ± 1^{c}	73 ± 1^{c}
KLD12	57 ± 4^{d}	60 ± 4^{d}	$59 \pm 5^{c,d}$

Mean ± standard error of the mean; [a,b,c,d,] versus day 7, day 14, agarose, and RAD, respectively, $p < 0.05$.

Hydrogel histology—accumulation of proteoglycans and collagen types I and II

Spatially uniform, metachromatic staining for the presence of sGAG was observed throughout both RAD16-I and KLD12 peptide hydrogels by day 21; in agarose, however, staining was largely confined to the immediate pericellular matrix (Fig. 4A). Positive type II collagen staining was also more intense and uniformly distributed throughout the RAD16-I and KLD12 peptide hydrogels than in the agarose, where again it was mainly in the pericellular matrix (Fig. 4B). Less intense nonuniform type I collagen staining was also visible in both peptide hydrogels, primarily in cell-associated regions, whereas little or no staining was seen in agarose hydrogels (Fig. 4C).

Aggrecan Western blot

GuHCl extracts from all three hydrogels revealed the presence of a large macromolecular species as detected by anti-G1 aggrecan Western blotting, running at the molecular weight of full-length aggrecan (>250 kDa, Fig. 5A). In both RAD16-I and KLD12 hydrogels, this full-length aggrecan was the predominant species detected, whereas in agarose hydrogels a doublet band near 65 kDa was the major immunoreactive product detected. The 65 kDa species was confirmed to be the aggrecanase-generated NITEGE neoepitope (Fig. 5B), suggesting the virtual absence of aggrecanase activity in the peptide gels in contrast with high aggrecanase activity in agarose. Since the agarose hydrogels nonetheless accumulated quite high levels of sGAG, it is possible that chondroitin sulfate (CS)-rich, non-G1–containing catabolic products of aggrecanase activity are retained in agarose, whereas these cleavage products are normally lost from cartilage explants.[45]

Cell and actin morphology

Spherical, isolated, uniformly seeded cells were observed in all the three scaffolds immediately after casting on day 0 (Fig. 6A) in both medium conditions (+TGF-β1 and Cntl). By day 4 in TGF-β1-supplemented medium, distinct morphologies were apparent in each of the hydrogels (Fig. 6B). Cell–cell contact appeared to be a feature for both peptide hydrogels with a spread, networked morphology in RAD16-I peptide and a clustered morphology in KLD12 peptide. In control medium, cell spreading and apparent cell–cell contact were observed in both peptide hydrogels, similar to but less extensive than the respective +TGF-β1 conditions (data not shown). At day 4, cells in agarose in both medium conditions maintained the same spherical, isolated morphology as at day 0, suggesting that these cells did not reorganize their actin cytoskeleton (Fig. 6B). Despite these early differences, cells in all the three hydrogels cultured with TGF-β1 had a more chondrocyte-like rounded morphology by day 21 (Fig. 6C), showing that the apparent cell–cell contact seen at day 4 in peptide hydrogels was a temporary feature. Using confocal microscopy, this predominantly rounded cell morphology was confirmed for all the three scaffolds at day 21 (Fig. 2D). To investigate the differences in BMSC morphol-

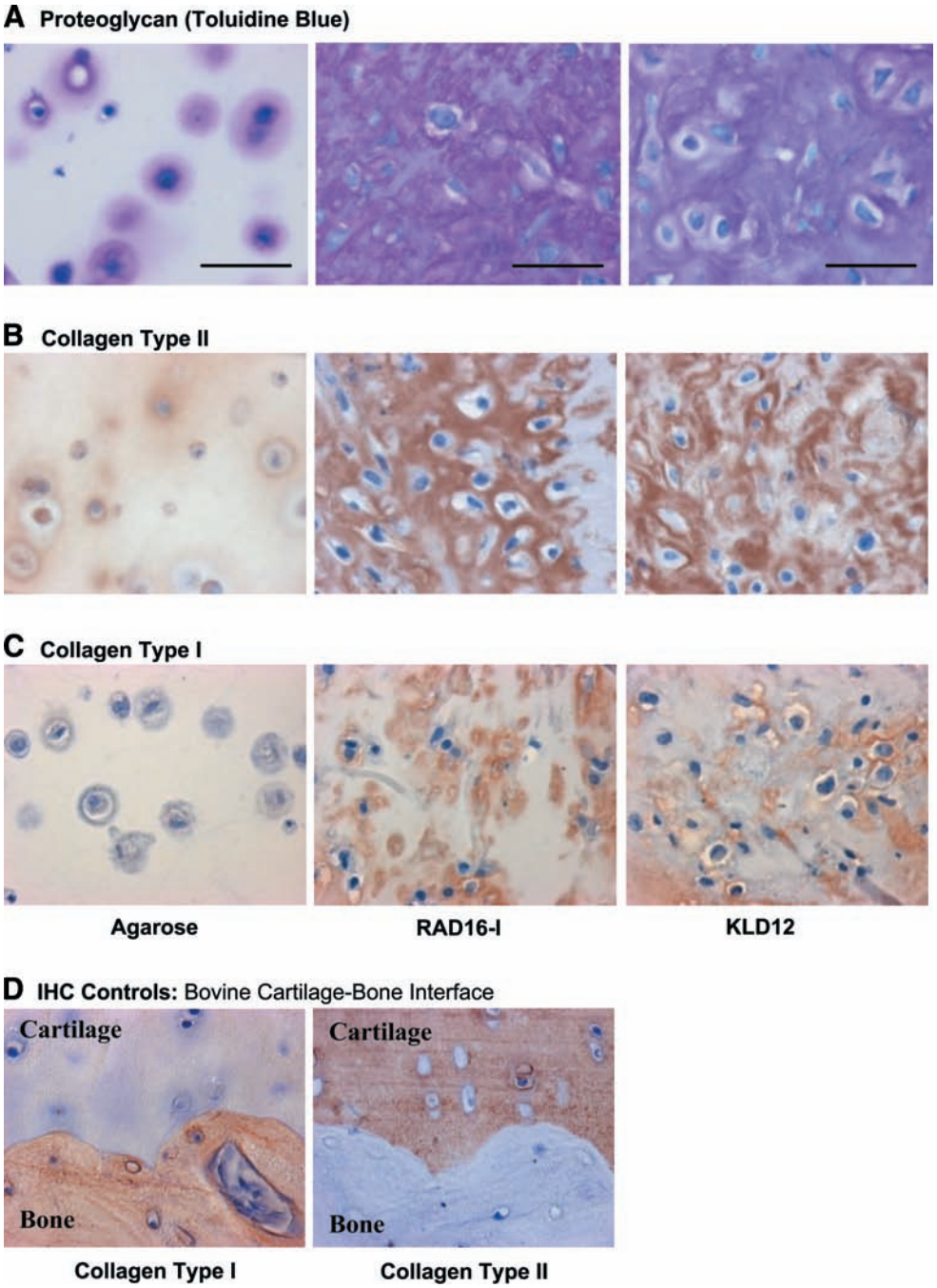

FIG. 4. Representative Toluidine Blue staining for (**A**) sulfated glycosaminoglycan, and (**B**) collagen type II and (**C**) type I immunohistochemistry images for BMSCs cultured with TGF-β1 supplementation in agarose (left column), RAD16-I (center column), and KLD12 (right column). (See "Materials and Methods" for details.) Culture duration was 21 days. (**D**) Collagen types I and II immunohistochemistry in bovine cartilage–bone plugs as controls. Scale bar in (**A**) is applicable to (**B**), (**C**), and (**D**), in all cases scale bar = 50 μm. Color images available online at www.liebertonline.com/ten.

ogy in RAD16-I and KLD12 hydrogel culture further, BMSCs were seeded onto polystyrene surfaces with adsorbed RAD16-I or KLD12 peptide monomers. After 2 h, cells attached and spread to a significantly greater degree on RAD16-I surfaces than KLD12 (Fig. 7A). Quantitative image analysis showed greater numbers of attaching cells per field, and more than double the area per cell, on RAD16-I peptide than on KLD12 surfaces (Fig. 7B).

Discussion

The capacity for self-assembling peptide hydrogels to support and enhance chondrogenesis of 3D-encapsulated BMSCs was compared with that in agarose hydrogel culture. Both the DNA content and the accumulation of a cartilage-like ECM were higher for TGF-β1-stimulated BMSCs in RAD16-I and KLD12 hydrogels than in agarose. Several recent reports have shown similar concomitant increases in ECM production and BMSC proliferation in pellet culture[46] as well as with encapsulation in agarose[47,48] and polyethylene glycol (PEG) hydrogels[49] through manipulation of the cellular microenvironment. Due to compaction of both peptide hydrogels, but not agarose, normalization of data to wet mass (Fig. 3) would exaggerate the higher DNA content and ECM accumulation for peptide hydrogels. Thus, the motivation for presenting the data on a per-hydrogel sample

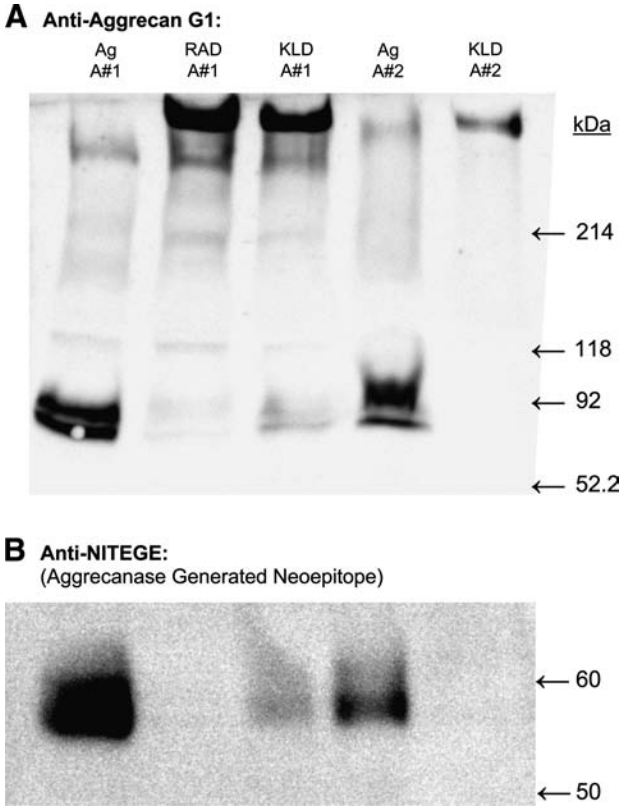

FIG. 5. Aggrecan Western blot. Aggrecan extracted from BMSC-seeded agarose (Ag), RAD16-I (RAD), or KLD12 (KLD) hydrogels after 21 days in culture with TGF-β1 supplementation. Lanes 1–3 extracted from animal #1; lanes 4 and 5 extracted from animal #2. (**A**) Anti-aggrecan G1. (**B**) Anti-NITEGE (aggrecanase generated neoepitope).

basis was to allow for a direct comparison of the neotissue construct in each hydrogel given an equal initial cell content and hydrogel size. The results are consequently consistent with a recent report where wet mass-normalized KLD12 peptide hydrogels had higher sGAG content than agarose hydrogels,[23] but are in contrast with the findings of Erickson *et al.*,[22] which report higher sGAG content in agarose than in RAD16-I hydrogels.

Two major chondrogenic ECM genes, type II collagen and aggrecan, were upregulated by over three orders of magnitude in all three hydrogels in the presence of TGF-β1 (Fig. 2). Consistent with recent reports on chondrogenesis of BMSCs in pellet,[50,51] agarose,[5,52] PEG,[30] and alginate[6,53] culture, the sharpest increases in mRNA transcript levels for type II collagen and aggrecan occurred during the first 3–7 days of culture, and transcript levels were nearly flat during the second week of culture (Fig. 2). Type I collagen, an important ECM molecule during early chondrogenesis in the developing limb bud,[28,29] was upregulated at day 4 with TGF-β1, but by substantially less than either type II collagen or aggrecan. SOX9 transcript levels were an order of magnitude higher with TGF-β1 by day 7, also consistent with recent reports in alginate.[6,30] Markers for osteogenesis (osteocalcin) and adipogenesis (PPAR-γ) were unchanged from their day 0 undifferentiated values in the presence of TGF-β1, demonstrating specific chondrogenic differentiation. Given that changes in cell morphology, hydrogel compaction, and the resulting cell–cell contacts occurred in peptide hydrogels during the first week of culture, and that concomitant upregulation of chondrogenic genes occurred in both agarose and peptide hydrogels during the first week, it is likely that critical cell differentiation decisions occur within the first few days after BMSC encapsulation in 3D culture and exposure to TGF-β1.

sGAG retention in agarose hydrogels dropped dramatically in the final week of culture but was maintained in both peptides. This is in contrast to sGAG release from chondrocyte-seeded agarose cultures, which is constant over time,[34] but consistent with our results showing no additional accumulation of sGAG in agarose in the final week. sGAG accumulation in both peptide hydrogels, however, significantly increased during this time. Thus, while BMSCs in agarose and peptide hydrogels had similar DNA-normalized proteoglycan synthesis rates, the sGAG produced in agarose cultures was preferentially lost to the medium while that in peptide cultures was retained. This was consistent with the Toluidine Blue staining that indicated more uniform negative charge content in the peptide gels compared with agarose cultures. The potential mechanisms for these differences in sGAG retention may be catabolic (i.e., the action of proteases cleaving aggrecan and thereby increasing release of sGAG) or antianabolic (i.e., the relative lack of production of ECM components necessary for aggrecan–sGAG retention such as link protein and/or hyaluronan, or the lower ECM density in agarose due to compaction differences). To further understand the relative importance of these contrasting mechanisms, Western analysis with anti-G1 aggrecan antiserum and anti-NITEGE neoepitope antibody was performed on hydrogel protein extracts (Fig. 5A, B). Results showed a doublet at ~65 kDa as the dominant product in the agarose hydrogels samples only, which was confirmed to be the aggrecanase-generated NITEGE neoepitope–containing fragment.[45] Thus, an apparent high level of catabolic enzyme activity may have led to the observed decrease in sGAG retention in agarose, suggesting an important difference between the chondrogenic programs executed in agarose and peptide hydrogels or an anticatabolic property of the peptide hydrogel scaffolds.

The three distinct cytoskeletal morphologies observed during the first week of culture suggest that unique biophysical signals are generated in each hydrogel. The mechanisms responsible for these differing cell morphologies are not known but may include the state of differentiation of the cells, the scaffold mechanical stiffness, and cell–scaffold adhesion.[28] For example, the equilibrium modulus of 2% agarose is ~10 kPa,[34,35] which is approximately 10-fold higher than RAD16-I (~1 kPa storage modulus),[19] while RAD16-I and KLD12 have stiffness values within 25% of each other.[20] The stiffer agarose thus likely confines cells to a spherical morphology and prevents cell-mediated hydrogel compaction, consistent with recent reports in which BMSC-seeded 2% agarose maintained nearly constant volume and did not compact during long-term culture.[4,22] To test this hypothesis, we reduced the agarose concentration to 0.5%, which reduces the compressive modulus to the same order of magnitude as both peptides.[35] BMSCs seeded into this 0.5% agarose compacted hydrogels by 69% supporting the concept that hydrogel mechanical properties can be important in

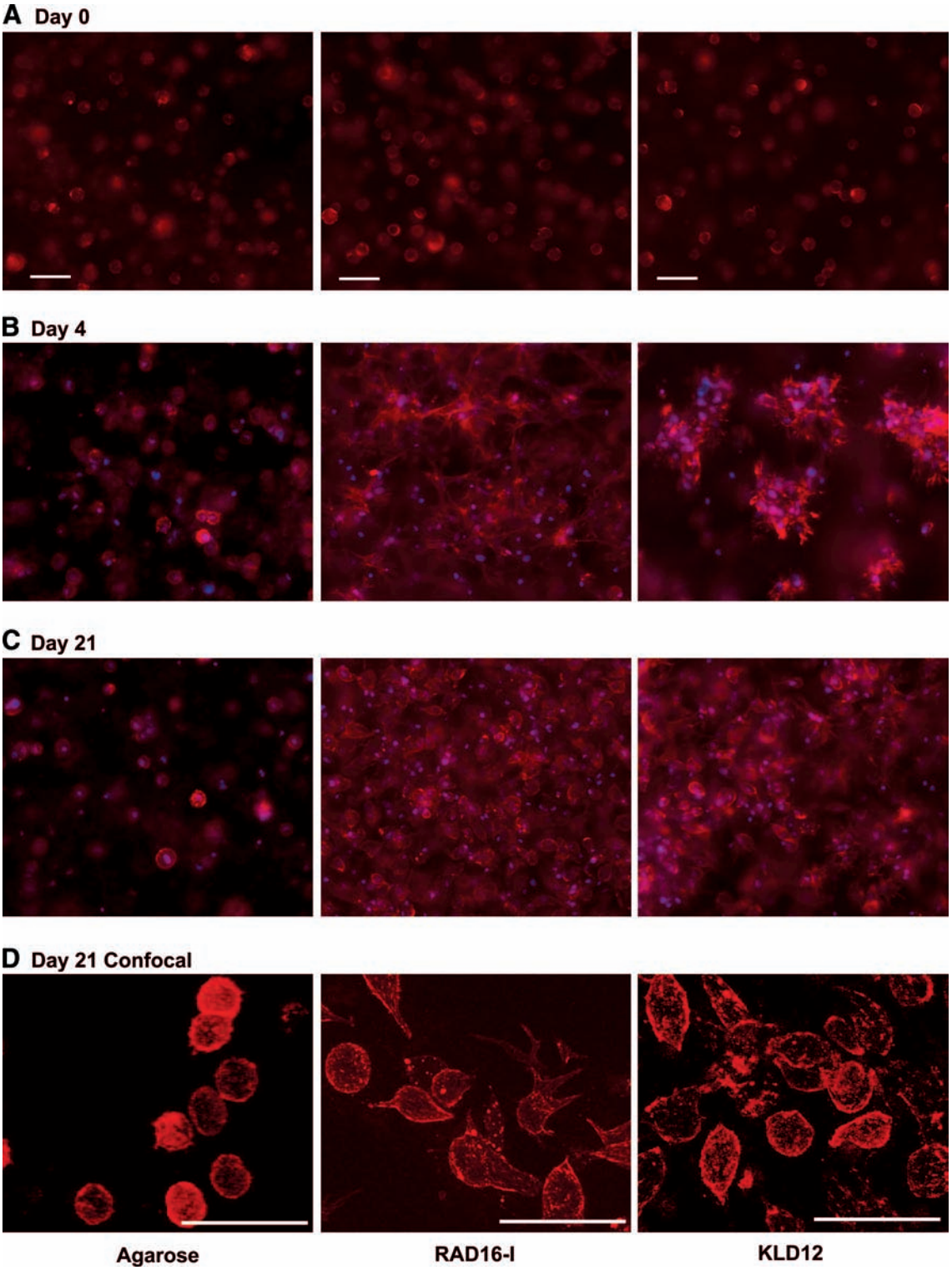

FIG. 6. Representative three-dimensional F-actin morphology images for BMSCs cultured with TGF-β1 supplementation and encapsulated in agarose (left column), RAD16-I (center column), and KLD12 (right column). Culture duration was (**A**) 0 days, (**B**) 4 days, or (**C**) 21 days. (**D**) High magnification, confocal images at day 21. Red indicates F-actin and blue indicates cell nuclei. Scale bar in (**A**) is applicable to (**B**) and (**C**), in all cases scale bar = 50 μm. Color images available online at www.liebertonline.com/ten.

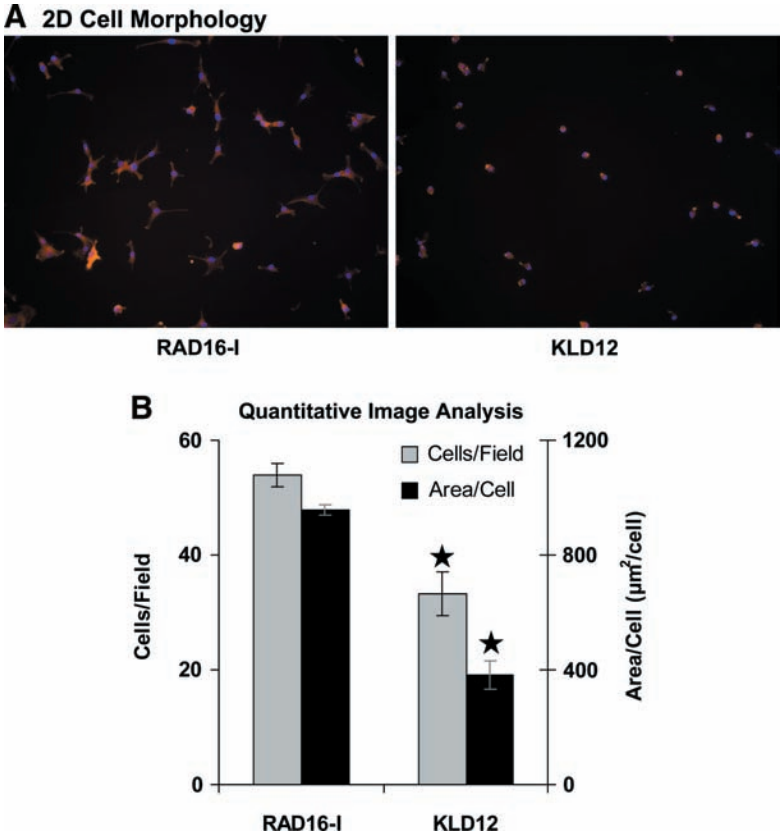

FIG. 7. (**A**) Representative 2D F-actin morphology for BMSCs seeded onto RAD16-I (left) and KLD12 (right) surfaces for 2 h. Red indicates F-actin and blue indicates cell nuclei. (**B**) Quantification of 2D images. Values shown are mean ± standard error of the mean; $n = 5$ fields, field area $= 5.61 \times 10^{-3}$ cm^2, ⋆ versus RAD16-I, $p < 0.01$. Color images available online at www.liebertonline.com/ten.

this system. However, since cell–scaffold interactions are likely not significant in agarose, this result suggests that the newly secreted ECM or cell–cell interactions may be involved in hydrogel compaction in the agarose system.

Since the stiffness of RAD16-I and KLD12 is similar,[20] differences in cell–scaffold adhesion or cell differentiation are likely more important for explaining the differences between the network of cell–cell contacts observed in RAD16-I and the multicell clusters in KLD12. To investigate this possibility, BMSCs were seeded onto 2D peptide-coated surfaces. More cells per field and greater spread area per cell were observed for BMSCs on RAD16-I than on KLD12 during 2-h adhesion experiments (Fig. 7). A recent report on human umbilical vein endothelial cell (HUVEC) adhesion and spreading on RAD16-I and KLD12 hydrogels[19] also showed more cells attaching and greater spreading per cell when seeded on RAD16-I compared with KLD12 hydrogels. These differences in adhesion are consistent with the 3D scaffold effects observed here, where more intimate cell–scaffold contact created by the network morphology in RAD16-I may be due to greater cell–scaffold adhesion, whereas cell clusters in KLD12 may result from weaker cell–scaffold interactions.

Despite these peptide-sequence-specific morphological differences, we were not able to quantify differences in chondrogenesis by the measurement of cartilage gene expression or ECM production in this study. Nonetheless, the importance of the cell microenvironment niche in BMSC differentiation state[54] suggests that differences in chondrogenesis likely exist given the dramatic contrast between spread network and clustered morphology in RAD16-I and KLD12, respectively. Due to the microenvironment control provided by modulating peptide sequence, these hydrogels are a powerful tool for the study of the BMSC niche and chondrogenesis. Further as understanding is gained about how the BMSC microenvironment affects chondrogenesis, self-assembling peptides can be functionalized with adhesion and signaling motifs[55,56] to enable precise control of progenitor cell differentiation.[55,57]

Two features seen in common to both peptides, but not 2% agarose, were hydrogel compaction and extensive cell–cell contact. In a recent review of biophysical signals in prenatal chondrogenic condensations, Knothe Tate *et al.*[28] reported that increasing cell density and cell–cell contact stimulates mitotic activity. Further, the formation of cell condensations amplifies the number of cells that subsequently undergo overt chondrogenesis.[58,59] Thus, greater cell proliferation in both RAD16-I and KLD12 peptide hydrogels compared with agarose, as evidenced by higher DNA content, may be stimulated by cell–cell contact and the increased cell density generated by compaction of the peptide scaffolds. Interestingly, a similar effect of compaction-stimulated mitotic activity was observed for chondrocytes seeded in a collagen–GAG scaffold.[60]

The importance of scaffold design in promoting chondrogenesis of BMSCs for cartilage tissue engineering has been demonstrated in this study via differences in ECM protein production, retention, and cell morphology. Peptide hydrogels enhanced early chondrogenesis compared with

agarose, and unique signals generated by each peptide sequence subtly altered the chondrogenic differentiation program. In addition to the importance of scaffold-generated, biophysical signals, TGF-β1 was a critical biochemical signal necessary to promote chondrogenesis. By further optimizing self-assembling peptide hydrogels, it may be possible to incorporate biochemical signals into the scaffold.[26] Additionally, self-assembling peptide hydrogels can successfully facilitate the generation of cartilage neotissue when seeded with an adult equine BMSC source[23,61] as well as the newborn bovine BMSC source described here. Thus, these materials have the potential to incorporate both the appropriate biophysical and biochemical chondrogenic stimuli for multiple species and ages, making them a promising candidate scaffold for use in a clinically feasible, cartilage repair therapy.

Acknowledgments

The authors would like to thank Hsu-Yi Lee for performing the quantitative image analysis of 2D BMSC morphology. This work was funded by the National Institutes of Health (NIH EB003805), a National Institutes of Health Molecular, Cell, and Tissue Biomechanics Training Grant Fellowship (P.W.K.), and an Arthritis Foundation Postdoctoral Fellowship (E.J.V.).

Disclosure Statement

No competing financial interests exist.

References

1. Pittenger, M.F., Mackay, A.M., Beck, S.C., Jaiswal, R.K., Douglas, R., Mosca, J.D., Moorman, M.A., Simonetti, D.W., Craig, S., and Marshak, D.R. Multilineage potential of adult human mesenchymal stem cells. Science **284,** 143, 1999.
2. Johnstone, B., Hering, T.M., Caplan, A.I., Goldberg, V.M., and Yoo, J.U. *In vitro* chondrogenesis of bone marrow-derived mesenchymal progenitor cells. Exp Cell Res **238,** 265, 1998.
3. Noth, U., Steinert, A.F., and Tuan, R.S. Technology insight: adult mesenchymal stem cells for osteoarthritis therapy. Nat Clin Pract Rheumatol **4,** 371, 2008.
4. Mauck, R.L., Yuan, X., and Tuan, R.S. Chondrogenic differentiation and functional maturation of bovine mesenchymal stem cells in long-term agarose culture. Osteoarthritis Cartilage **14,** 179, 2006.
5. Mouw, J.K., Connelly, J.T., Wilson, C.G., Michael, K.E., and Levenston, M.E. Dynamic compression regulates the expression and synthesis of chondrocyte-specific matrix molecules in bone marrow stromal cells. Stem Cells **25,** 655, 2007.
6. Connelly, J.T., Garcia, A.J., and Levenston, M.E. Inhibition of *in vitro* chondrogenesis in RGD-modified three-dimensional alginate gels. Biomaterials **28,** 1071, 2007.
7. Hui, T.Y., Cheung, K.M., Cheung, W.L., Chan, D., and Chan, B.P. *In vitro* chondrogenic differentiation of human mesenchymal stem cells in collagen microspheres: influence of cell seeding density and collagen concentration. Biomaterials **29,** 3201, 2008.
8. Schulz, R.M., Zscharnack, M., Hanisch, I., Geiling, M., Hepp, P., and Bader, A. Cartilage tissue engineering by collagen matrix associated bone marrow derived mesenchymal stem cells. Biomed Mater Eng **18,** S55, 2008.
9. Mohan, N., Nair, P.D., and Tabata, Y. A 3D biodegradable protein based matrix for cartilage tissue engineering and stem cell differentiation to cartilage. J Mater Sci Mater Med 2008, PMID: 18560767.
10. Haider, M., Cappello, J., Ghandehari, H., and Leong, K.W. *In vitro* chondrogenesis of mesenchymal stem cells in recombinant silk-elastinlike hydrogels. Pharm Res **25,** 692, 2008.
11. Steinert, A.F., Ghivizzani, S.C., Rethwilm, A., Tuan, R.S., Evans, C.H., and Noth, U. Major biological obstacles for persistent cell-based regeneration of articular cartilage. Arthritis Res Ther **9,** 213, 2007.
12. Tuan, R.S. Stemming cartilage degeneration: adult mesenchymal stem cells as a cell source for articular cartilage tissue engineering. Arthritis Rheum **54,** 3075, 2006.
13. Raghunath, J., Rollo, J., Sales, K.M., Butler, P.E., and Seifalian, A.M. Biomaterials and scaffold design: key to tissue-engineering cartilage. Biotechnol Appl Biochem **46,** 73, 2007.
14. Rajangam, K., Behanna, H.A., Hui, M.J., Han, X., Hulvat, J.F., Lomasney, J.W., and Stupp, S.I. Heparin binding nanostructures to promote growth of blood vessels. Nano Lett **6,** 2086, 2006.
15. Haines-Butterick, L., Rajagopal, K., Branco, M., Salick, D., Rughani, R., Pilarz, M., Lamm, M.S., Pochan, D.J., and Schneider, J.P. Controlling hydrogelation kinetics by peptide design for three-dimensional encapsulation and injectable delivery of cells. Proc Natl Acad Sci USA **104,** 7791, 2007.
16. Zhang, S., Holmes, T., Lockshin, C., and Rich, A. Spontaneous assembly of a self-complementary oligopeptide to form a stable macroscopic membrane. Proc Natl Acad Sci USA **90,** 3334, 1993.
17. Holmes, T.C. Novel peptide-based biomaterial scaffolds for tissue engineering. Trends Biotechnol **20,** 16, 2002.
18. Caplan, M.R., Schwartzfarb, E.M., Zhang, S., Kamm, R.D., and Lauffenburger, D.A. Effects of systematic variation of amino acid sequence on the mechanical properties of a self-assembling, oligopeptide biomaterial. J Biomater Sci Polym Ed **13,** 225, 2002.
19. Sieminski, A.L., Was, A.S., Kim, G., Gong, H., and Kamm, R.D. The stiffness of three-dimensional ionic self-assembling peptide gels affects the extent of capillary-like network formation. Cell Biochem Biophys **49,** 73, 2007.
20. Sieminski, A.L., Semino, C.E., Gong, H., and Kamm, R.D. Primary sequence of ionic self-assembling peptide gels affects endothelial cell adhesion and capillary morphogenesis. J Biomed Mater Res A **87,** 494, 2008.
21. Kisiday, J., Jin, M., Kurz, B., Hung, H., Semino, C., Zhang, S., and Grodzinsky, A.J. Self-assembling peptide hydrogel fosters chondrocyte extracellular matrix production and cell division: implications for cartilage tissue repair. Proc Natl Acad Sci USA **99,** 9996, 2002.
22. Erickson, I.E., Huang, A.H., Chung, C., Li, R.T., Burdick, J.A., and Mauck, R.L. Differential maturation and structure-function relationships in MSC- and chondrocyte-seeded hydrogels. Tissue Eng Part A 2009.
23. Kisiday, J.D., Kopesky, P.W., Evans, C.H., Grodzinsky, A.J., McIlwraith, C.W., and Frisbie, D.D. Evaluation of adult equine bone marrow- and adipose-derived progenitor cell chondrogenesis in hydrogel cultures. J Orthop Res **26,** 322, 2008.
24. Semino, C.E., Merok, J.R., Crane, G.G., Panagiotakos, G., and Zhang S. Functional differentiation of hepatocyte-like spheroid structures from putative liver progenitor cells in three-dimensional peptide scaffolds. Differentiation **71,** 262, 2003.

25. Wang, S., Nagrath, D., Chen, P.C., Berthiaume, F., and Yarmush, M.L. Three-dimensional primary hepatocyte culture in synthetic self-assembling peptide hydrogel. Tissue Eng **14,** 227, 2008.
26. Davis, M.E., Hsieh, P.C., Takahashi, T., Song, Q., Zhang, S., Kamin, R.D., Grodzinsky, A.J., Anversa, P., and Lee, R.T. Local myocardial insulin-like growth factor 1 (IGF-1) delivery with biotinylated peptide nanofibers improves cell therapy for myocardial infarction. Proc Natl Acad Sci USA **103,** 8155, 2006.
27. Miller, R., Grodzinsky, A., Vanderploeg, E., Kopesky, P., Florine, E., Barrett, M., Ferris, D., Kisiday, J., and Frisbie, D. Self-assembling peptide heals rabbit defects *in vivo*. In: Proceedings of the 2009 OARSI World Congress on Osteoarthritis, Montreal, Canada, September 10–13, 2009.
28. Knothe Tate, M.L., Falls, T.D., McBride, S.H., Atit, R., and Knothe, U.R. Mechanical modulation of osteochondroprogenitor cell fate. Int J Biochem Cell Biol **40,** 2720, 2008.
29. Goldring, M.B., Tsuchimochi, K., and Ijiri, K. The control of chondrogenesis. J Cell Biochem **97,** 33, 2006.
30. Varghese, S., Hwang, N.S., Canver, A.C., Theprungsirikul, P., Lin, D.W., and Elisseeff, J. Chondroitin sulfate based niches for chondrogenic differentiation of mesenchymal stem cells. Matrix Biol **27,** 12, 2008.
31. Kamiya, N., Watanabe, H., Habuchi, H., Takagi, H., Shinomura, T., Shimizu, K., and Kimata, K. Versican/PG-M regulates chondrogenesis as an extracellular matrix molecule crucial for mesenchymal condensation. J Biol Chem **281,** 2390, 2006.
32. Connelly, J.T., Wilson, C.G., and Levenston, M.E. Characterization of proteoglycan production and processing by chondrocytes and BMSCs in tissue engineered constructs. Osteoarthritis Cartilage **16,** 1092, 2008.
33. Chung, C., and Burdick, J.A. Influence of three-dimensional hyaluronic acid microenvironments on mesenchymal stem cell chondrogenesis. Tissue Eng Part A **15,** 243, 2009.
34. Buschmann, M.D., Gluzband, Y.A., Grodzinsky, A.J., Kimura, J.H., and Hunziker, E.B. Chondrocytes in agarose culture synthesize: a mechanically functional extracellular matrix. J Orthop Res 10, 745, 1992.
35. Mauck, R.L., Soltz, M.A., Wang, C.C., Wong, D.D., Chao, P.H., Valhmu, W.B., Hung, C.T., and Ateshian, G.A. Functional tissue engineering of articular cartilage through dynamic loading of chondrocyte-seeded agarose gels. J Biomech Eng **122,** 252, 2000.
36. Benya, P.D., and Shaffer, J.D. Dedifferentiated chondrocytes reexpress the differentiated collagen phenotype when cultured in agarose gels. Cell **30,** 215, 1982.
37. Domm, C., Schunke, M., Christesen, K., and Kurz, B. Redifferentiation of dedifferentiated bovine articular chondrocytes in alginate culture under low oxygen tension. Osteoarthritis Cartilage **10,** 13, 2002.
38. Fitzgerald, J.B., Jin, M., Dean, D., Wood, D.J., Zheng, M.H., and Grodzinsky, A.J. Mechanical compression of cartilage explants induces multiple time-dependent gene expression patterns and involves intracellular calcium and cyclic AMP. J Biol Chem **279,** 19502, 2004.
39. Bosnakovski, D., Mizuno, M., Kim, G., Takagi, S., Okumura, M., and Fujinaga, T. Isolation and multilineage differentiation of bovine bone marrow mesenchymal stem cells. Cell Tissue Res **319,** 243, 2005.
40. Pfaffl, M.W. A new mathematical model for relative quantification in real-time RT-PCR. Nucleic Acids Res **29,** e45, 2001.
41. Farndale, R.W., Sayers, C.A., and Barrett, A.J. A direct spectrophotometric microassay for sulfated glycosaminoglycans in cartilage cultures. Connect Tissue Res **9,** 247, 1982.
42. Kim, Y.J., Sah, R.L., Doong, J.Y., and Grodzinsky, A.J. Fluorometric assay of DNA in cartilage explants using Hoechst 33258. Anal Biochem **174,** 168, 1988.
43. Ng, L., Grodzinsky, A.J., Patwari, P., Sandy, J., Plaas, A., and Ortiz, C. Individual cartilage aggrecan macromolecules and their constituent glycosaminoglycans visualized via atomic force microscopy. J Struct Biol **143,** 242, 2003.
44. Chockalingam, P.S., Zeng, W., Morris, E.A., and Flannery, C.R. Release of hyaluronan and hyaladherins (aggrecan G1 domain and link proteins) from articular cartilage exposed to ADAMTS-4 (aggrecanase 1) or ADAMTS-5 (aggrecanase 2). Arthritis Rheum **50,** 2839, 2004.
45. Patwari, P., Kurz, B., Sandy, J.D., and Grodzinsky, A.J. Mannosamine inhibits aggrecanase-mediated changes in the physical properties and biochemical composition of articular cartilage. Arch Biochem Biophys **374,** 79, 2000.
46. Hardingham, T.E., Oldershaw, R.A., and Tew, S.R. Cartilage, SOX9 and notch signals in chondrogenesis. J Anat **209,** 469, 2006.
47. Connelly, J.T., Garcia, A.J., and Levenston, M.E. Interactions between integrin ligand density and cytoskeletal integrity regulate BMSC chondrogenesis. J Cell Physiol **217,** 145, 2008.
48. Shintani, N., and Hunziker, E.B. Chondrogenic differentiation of bovine synovium: bone morphogenetic proteins 2 and 7 and transforming growth factor beta1 induce the formation of different types of cartilaginous tissue. Arthritis Rheum **56,** 1869, 2007.
49. Hwang, N.S., Varghese, S., Lee, H.J., Zhang, Z., Ye, Z., Bae, J., Cheng, L., and Elisseeff, J. *In vivo* commitment and functional tissue regeneration using human embryonic stem cell-derived mesenchymal cells. Proc Natl Acad Sci USA **105,** 20641, 2008.
50. Barry, F., Boynton, R.E., Liu, B., and Murphy, J.M. Chondrogenic differentiation of mesenchymal stem cells from bone marrow: differentiation-dependent gene expression of matrix components. Exp Cell Res **268,** 189, 2001.
51. Bosnakovski, D., Mizuno, M., Kim, G., Takagi, S., Okumur, M., and Fujinag, T. Gene expression profile of bovine bone marrow mesenchymal stem cell during spontaneous chondrogenic differentiation in pellet culture system. Jpn J Vet Res **53,** 127, 2006.
52. Huang, C.Y., Hagar, K.L., Frost, L.E., Sun, Y., and Cheung, H.S. Effects of cyclic compressive loading on chondrogenesis of rabbit bone-marrow derived mesenchymal stem cells. Stem Cells **22,** 313, 2004.
53. Bosnakovski, D., Mizuno, M., Kim, G., Takagi, S., Okumura, M., and Fujinaga, T. Chondrogenic differentiation of bovine bone marrow mesenchymal stem cells (MSCs) in different hydrogels: influence of collagen type II extracellular matrix on MSC chondrogenesis. Biotechnol Bioeng **93,** 1152, 2006.
54. Eckfeldt, C.E., Mendenhall, E.M., and Verfaillie, C.M. The molecular repertoire of the "almighty" stem cell. Nat Rev Mol Cell Biol **6,** 726, 2005.
55. Gelain, F., Bottai, D., Vescovi, A., and Zhang, S. Designer self-assembling peptide nanofiber scaffolds for adult mouse neural stem cell 3-dimensional cultures. PLoS ONE **1,** e119, 2006.
56. Genove, E., Shen, C., Zhang, S., and Semino, C.E. The effect of functionalized self-assembling peptide scaffolds on

human aortic endothelial cell function. Biomaterials **26,** 3341, 2005.
57. Horii, A., Wang, X., Gelain, F., and Zhang, S. Biological designer self-assembling peptide nanofiber scaffolds significantly enhance osteoblast proliferation, differentiation and 3-D migration. PLoS ONE **2,** e190, 2007.
58. Hall, B.K., and Miyake, T. Divide, accumulate, differentiate: cell condensation in skeletal development revisited. Int J Dev Biol **39,** 881, 1995.
59. Hall, B.K., and Miyake, T. All for one and one for all: condensations and the initiation of skeletal development. Bioessays **22,** 138, 2000.
60. Lee, C.R., Grodzinsky, A.J., and Spector, M. Modulation of the contractile and biosynthetic activity of chondrocytes seeded in collagen-glycosaminoglycan matrices. Tissue Eng **9,** 27, 2003.
61. Kopesky, P., Lee, C.S.D., Miller, R.E., Kisiday, J.D., Frisbie, D.D., and Grodzinsky, A.J. Comparable matrix production by adult equine marrow-derived MSCs and primary chondrocytes in a self-assembling peptide hydrogel: effect of age and growth factors. Presented at the 53rd Orthopedic Research Society, San Diego, CA, February 11–14, 2007.

Address correspondence to:
Alan J. Grodzinsky, Sc.D.
Center for Biomedical Engineering
MIT
MIT Room NE47-377
Cambridge, MA 02139

E-mail: alg@mit.edu

Received: March 7, 2009
Accepted: August 24, 2009
Online Publication Date: October 2, 2009